



# NIH Public Access

## Author Manuscript

*Biochemistry*. Author manuscript; available in PMC 2011 October 4.

Published in final edited form as:

*Biochemistry*. 2010 April 13; 49(14): 3116–3128. doi:10.1021/bi100115a.

## N-Glycan-Dependent Quality Control of the Na,K-ATPase $\beta_2$ Subunit<sup>†</sup>

Elmira Tokhtaeva, Keith Munson, George Sachs, and Olga Vagin\*

Department of Physiology, School of Medicine, UCLA, and Veterans Administration Greater Los Angeles Health Care System, VAGLAHS/West LA, Building 113, Room 324, 11301 Wilshire Boulevard, Los Angeles, California 90073

### Abstract

Bulky hydrophilic N-glycans stabilize the proper tertiary structure of glycoproteins. In addition, N-glycans comprise the binding sites for the endoplasmic reticulum (ER)-resident lectins that assist correct folding of newly synthesized glycoproteins. To reveal the role of N-glycans in maturation of the Na,K-ATPase  $\beta_2$  subunit in the ER, the effects of preventing or modifying the  $\beta_2$  subunit N-glycosylation on trafficking of the subunit and its binding to the ER lectin chaperone, calnexin, were studied in MDCK cells. Preventing N-glycosylation abolishes binding of the  $\beta_2$  subunit to calnexin and results in the ER retention of the subunit. Furthermore, the fully N-glycosylated  $\beta_2$  subunit is retained in the ER when glycan–calnexin interactions are prevented by castanospermine, showing that N-glycan-mediated calnexin binding is required for correct subunit folding. Calnexin binding persists for several hours after translation is stopped with cycloheximide, suggesting that the  $\beta_2$  subunit undergoes repeated post-translational calnexin-assisted folding attempts. Homology modeling of the  $\beta_2$  subunit using the crystal structure of the  $\alpha_1$ - $\beta_1$  Na,K-ATPase shows the presence of a relatively hydrophobic amino acid cluster proximal to N-glycosylation sites 2 and 7. Combined, but not separate, removal of sites 2 and 7 dramatically impairs calnexin binding and prevents the export of the  $\beta_2$  subunit from the ER. Similarly, hydrophilic substitution of two hydrophobic amino acids in this cluster disrupts both  $\beta_2$ –calnexin binding and trafficking of the subunit to the Golgi. Therefore, the hydrophobic residues in the proximity of N-glycans 2 and 7 are required for post-translational calnexin binding to these N-glycans in incompletely folded conformers, which, in turn, is necessary for maturation of the Na,K-ATPase  $\beta_2$  subunit.

---

The endoplasmic reticulum (ER) lumen contains high concentrations of molecular chaperones and folding enzymes that allow newly synthesized proteins to acquire their native conformation. Nevertheless, a large fraction of ER-synthesized proteins fail to fold properly on the first attempt. Cells overcome this problem by employing an ER-resident protein quality control system that includes a variety of proteins and operates on levels of protein synthesis, folding, and assembly. By preventing the premature exit of non-native

<sup>†</sup>Supported by National Institutes of Health Grants DK077149 and DK058333.

© 2010 American Chemical Society

\*To whom correspondence should be addressed. olgav@ucla.edu. Phone: (310) 268-3924. Fax: (310) 312-9478.

### SUPPORTING INFORMATION AVAILABLE

Sequences of primers used for mutations of N-glycosylation sites in YFP- $\beta_2$  (Table 1), sequences of primers used for mutations of amino acid residues next to N-glycan 7 in YFP- $\beta_2$  (Table 2), Western blot analysis of total lysates of the cells expressing the wild-type YFP-linked  $\beta_2$  subunit and its glycosylation-deficient mutants (Figure 1), and hydropathy of regions next to N-glycosylation sites in the  $\beta_2$  and  $\beta_1$  subunits of the Na,K-ATPase (Figure 2). The hydropathy plots of the  $\beta_2$  and  $\beta_1$  subunits were generated according to the method described in ref 40 with a window size of 9. The 15-amino acid regions downstream of each N-glycosylation site of the  $\beta_2$  and  $\beta_1$  subunits are shown. The numbering of N-glycosylation sites corresponds to that in Figure 5A. This material is available free of charge via the Internet at <http://pubs.acs.org>.

conformers and incompletely assembled proteins from the ER, the quality control system extends exposure of substrates to the folding machinery in the ER lumen and hence improves the chances of correct maturation. If proper folding or full assembly is not achieved even after repeated attempts, proteins are then moved from the ER to the cytosol and destroyed via the ER-associated degradation (ERAD)<sup>1</sup> pathway (1–3). Hence, the ER quality control system ensures that only properly folded and assembled proteins are exported to the Golgi to begin their travel to their final destinations. The importance of the ER quality control system in maintaining the fidelity of cellular functions is evidenced by many diseases, including cystic fibrosis, antitrypsin deficiency, Alzheimer's disease, and Huntington's disease, that are linked to defects in this system (3,4).

There are two major groups of ER chaperones, heat shock protein homologues (e.g., BiP, Hsp40, and Hsp90) and lectins (e.g., calnexin, calreticulin, and EDEM-1) (5–9). Correct folding of nonglycosylated proteins is assisted by the ER heat shock protein homologues that, in conjunction with luminal thiol oxidoreductases, mediate disulfide bond formation. These non-lectin chaperones also mediate quality control of nonglycosylated proteins by retarding the premature exit of incompletely folded or unassembled proteins and by targeting of misfolded proteins to ERAD (5). In addition to these non-lectin chaperones, N-glycosylated proteins, which represent the majority of ER-synthesized proteins, also utilize the lectin chaperone system to help mediate folding and quality control (5–9).

Lectin chaperones use the N-glycans of glycoproteins as molecular recognition sites to guide the newly synthesized proteins through highly ordered steps of maturation and quality control. Every lectin-assisted maturation step is coupled with a particular modification of the N-glycan structure that is catalyzed by ER-resident enzymes. In eukaryotic cells, glycoproteins acquire the N-linked glycans during the process of translocation and elongation of the polypeptide chain. First, a 14-saccharide core is transferred from the dolichol phosphate precursor to the asparagine (Asn) residue within the N-glycosylation site, a consensus Asn-X-Thr/Ser (X is any amino acid residue except Pro) sequence of a nascent protein. Immediately after covalent linkage of this core oligosaccharide, its terminal glucose residues are sequentially trimmed by ER glucosidases. Removal of two of the three glucose residues enables N-glycan binding to a membrane-bound lectin, calnexin, or its soluble homologue, calreticulin. Binding to calnexin (calreticulin) can occur cotranslationally while the protein is still associated with the translocon.

Calnexin forms a complex with the oxidoreductase, ERp57, which catalyzes formation of disulfide bonds in the protein (5,6). When the newly synthesized protein is released from calnexin, it meets one of three possible fates. If it is folded correctly, is exported to the Golgi, or assembles with its partner subunits, if any, and then is exported. If the protein is terminally misfolded, it is often recognized by EDEMS and/or by a non-lectin chaperone, BiP, that facilitates translocation of the protein to the cytoplasm and proteasome-mediated degradation (5). If the protein is slightly misfolded, it is reglycosylated by UGGT1 and binds again to calnexin for refolding. This cycle can be repeated several times (5,6).

Thus, UGGT1 acts as a conformation sensor. Proteomic analysis of calnexin-interacting proteins in embryonic fibroblasts from UGGT1-null mice shows that many proteins do not require UGGT1 for maturation and complete their folding program in one calnexin binding event (10). Other proteins exhibit accelerated dissociation from calnexin and impaired folding in UGGT1-null fibroblasts, indicating that these proteins normally undergo several cycles of interaction with calnexin, mediated by UGGT1(10). Some of these proteins must

<sup>1</sup>Abbreviations: ERAD, endoplasmic reticulum-associated degradation; UGGT1, UDP-glucose glycoprotein glucosyltransferase 1; YFP- $\beta_1$  and YFP- $\beta_2$ , fusion proteins of the yellow fluorescent protein and the Na,K-ATPase  $\beta_1$  subunit and  $\beta_2$  subunit, respectively.

be essential for mouse viability since disruption of the UGGT1 gene results in embryonic lethality (11).

Here, we present data showing that one of these essential proteins that requires post-translational calnexin binding for proper folding is the  $\beta_2$  subunit of the Na,K-ATPase. The Na,K-ATPase is a vital transport enzyme expressed in all animal tissues where it generates ion gradients responsible for membrane potential and solute symport or antiport, as well as mediating intercellular junctions and signal transduction (12–18).

The Na,K-ATPase consists of an  $\alpha$  subunit that is responsible for catalysis of ion transport and an N-glycosylated  $\beta$  subunit that is implicated in maturation and membrane targeting of the enzyme. There are four isoforms of the Na,K-ATPase  $\alpha$  subunit ( $\alpha_1$ ,  $\alpha_2$ ,  $\alpha_3$ , and  $\alpha_4$ ) and three isoforms of the Na,K-ATPase  $\beta$  subunit ( $\beta_1$ ,  $\beta_2$ , and  $\beta_3$ ) (19,20). Assembly of the  $\alpha$  and  $\beta$  subunits that occurs in the ER soon after their biosynthesis is essential for formation of the functional enzyme (21) and for the export of both subunits from the ER to the Golgi (22–25).

Expression in *Xenopus* oocytes showed that  $\alpha_1$ ,  $\beta_1$ , and  $\beta_3$  subunits of the Na,K-ATPase interact with BiP and this interaction is important for retention of unassembled  $\alpha_1$ ,  $\beta_1$ , and  $\beta_3$  subunits in the ER (26), implying the involvement of this non-lectin chaperone system in the ER quality control of these particular isoforms of Na,K-ATPase. The presence of three, eight, and two N-glycans on the Na,K-ATPase  $\beta_1$ ,  $\beta_2$ , and  $\beta_3$  subunits, respectively, also suggests the possible involvement of an ER lectin chaperone system in the folding of these subunits, their assembly with the  $\alpha$  subunit, and quality control of the  $\alpha$ - $\beta$  complex. However, prevention of N-glycosylation of the  $\beta_1$  subunit by tunicamycin or by mutations of all three N-glycosylation sites only slightly impairs assembly of the  $\alpha_1$ - $\beta_1$  complex (26,27), trafficking of the pump to the plasma membrane (16,28), or Na,K-ATPase activity (26,28–30). Similarly, prevention of N-glycosylation of the  $\beta_3$  subunit by tunicamycin or by mutations of both N-glycosylation sites does not impair trafficking of this subunit to the plasma membrane (31). These results suggest that N-glycans and hence glycan–lectin interactions are not critical for folding of the  $\beta_1$  and  $\beta_3$  subunits.

On the other hand, native N-glycosylation has been shown to be essential for normal trafficking of the homologous H,K-ATPase  $\beta$  subunit from the ER (32). The Na,K-ATPase  $\beta_2$  subunit is more homologous to the H,K-ATPase  $\beta$  subunit than to the Na,K-ATPase  $\beta_1$  and  $\beta_3$  subunits. Similar to the H,K-ATPase  $\beta$  subunit, the Na,K-ATPase  $\beta_2$  subunit has multiple N-glycosylation sites. However, the contribution of glycan–lectin interactions to folding, maturation, and quality control of the Na,K-ATPase  $\beta_2$  subunit has not been investigated.

In this study, canine renal MDCK cells were used as the expression system for YFP-linked  $\beta_1$  and  $\beta_2$  subunit isoforms of the Na,K-ATPase and their N-glycosylation-deficient mutants to test whether the ER lectin quality control system is involved in maturation of the proteins. The results indicate that at least two of the eight N-glycans of the  $\beta_2$  subunit as well as the hydrophobic amino acid cluster downstream to the seventh N-glycan are critical both for calnexin binding and for normal maturation and ER exit of the subunit, suggesting the involvement of UGGT1-induced post-translational calnexin binding in folding and quality control of this subunit. In contrast, maturation of the  $\beta_1$  subunit does not require post-translational calnexin binding.

## MATERIALS AND METHODS

### Construction of MDCK Stable Cell Lines

The fusion proteins with YFP linked to the N-terminus of the Na,K-ATPase rat  $\beta_1$  or human  $\beta_2$  subunit (YFP- $\beta_1$  and YFP- $\beta_2$ ) and the unglycosylated mutant of YFP- $\beta_1$  lacking all three N-glycosylation sites (N158Q/N193Q/N266Q) were constructed as described previously (16). N-Glycosylation-deficient mutants of YFP- $\beta_2$ , lacking one, several, or all eight N-glycosylation sites, were constructed by site-directed mutagenesis using the QuikChange mutagenesis kit (Stratagene) by substitution of an asparagine residue of an N-glycosylation site with glutamine. The mutagenic primers (Table 1 of the Supporting Information) were constructed using PrimerSelect, version 5.03. Stable MDCK cell lines expressing wild-type and mutated YFP- $\beta_1$  and YFP- $\beta_2$  were obtained as described previously (33).

### Cell Culture

Cells were grown in DMEM medium (Cellgro Mediatech) containing 4.5 g/L glucose, 2 mM L-glutamine, 8 mg/L phenol red, 100 units/mL penicillin, 0.1 mg/mL streptomycin, and 10% FBS unless specified otherwise.

### Confocal Microscopy

Confocal microscopy images were acquired using the Zeiss LSM 510 laser scanning confocal microscope and LSM 510, version 3.2.

### Primary Antibodies

The following monoclonal antibodies were used for immunoprecipitation and/or Western blot analysis: against the Na,K-ATPase  $\alpha_1$  subunit, clone C464.6 (Millipore); against GFP, clones 7.1 and 13.1, which also recognize YFP (Roche Diagnostics); against calnexin, clone TO-5 (Santa Cruz Biotechnology). Also, polyclonal antibodies against calnexin (Abcam), against BiP (Abcam), and against GFP that also recognize YFP (Clontech) were used.

### Immunofluorescent Staining of MDCK Cells

Cells were fixed by incubation with 3.75% formaldehyde in PBS for 15 min at 37 °C and permeabilized by incubation with 0.1% Triton X-100 for 5 min. Then cells were incubated with Dako Protein Block Serum-Free solution (Dako Corp.) for 30 min. Immunostaining of the Na,K-ATPase  $\alpha_1$  subunit was performed via a 1 h incubation with the monoclonal antibody against the Na,K-ATPase  $\alpha_1$  subunit followed by a 1 h incubation with Alexa633-conjugated anti-mouse antibody (Invitrogen).

### Transient Transfection of MDCK Cells with the Fluorescent Marker of the ER

Cells grown on glass-bottom microwell dishes (MatTek Corp.) were transfected with the plasmid encoding a fusion protein between *Discosoma* sp. red fluorescent protein and the marker of the ER, DsRed2-ER (Clontech), using the Lipofectamine 2000 transfection reagent (Invitrogen) according to the manufacturer's instructions. Confocal microscopy images of transfected cells were acquired 24–48 h after transfection.

### Immunoprecipitation

Monolayers of MDCK cells grown in two or three 35 mm<sup>2</sup> wells of a six-well plate were rinsed twice with ice-cold PBS and lysed by incubation with 200 µL of the following mixture per well: 150 mM NaCl in 50 mM Tris (pH7.5) containing 1% Nonidet P40, 0.5% sodium deoxycholate, and Complete Protease Inhibitor Cocktail, 1 tablet/50 mL (Roche Diagnostics). Cell extracts were clarified by centrifugation (15000g for 10 min) at 4 °C.

Then, the cell extracts were incubated with 50  $\mu$ L of the protein A–agarose or protein G–agarose suspension (Roche Diagnostics) in a total volume of 1 mL of lysis buffer at 4 °C with continuous rotation for at least 3 h (or overnight) to remove the components that nonspecifically bind to protein A or G. Protein A was used when immunoprecipitation was performed by using polyclonal antibodies against calnexin or YFP, while protein G was used when immunoprecipitation was performed by using monoclonal antibodies against YFP. The precleared supernatant was mixed with 1–3  $\mu$ L of the appropriate antibody and incubated with continuous rotation at 4 °C for 60 min. After addition of 50  $\mu$ L of the protein A–agarose or protein G–agarose suspension, the mixture was incubated at 4 °C with continuous rotation overnight. The bead–adherent complexes were washed three times on the beads. The bead–adherent complexes obtained from two or three wells were collected in one tube, and then proteins were eluted from the beads by incubation in 80–120  $\mu$ L of SDS–PAGE sample buffer [4% SDS, 0.05% bromophenol blue, 20% glycerol, and 1%  $\beta$ -mercaptoethanol in 0.1 M Tris (pH 6.8)] for 5 min at 80 °C. Proteins eluted from the beads were separated by SDS–PAGE and analyzed by Western blotting to detect immunoprecipitated and co-immunoprecipitated proteins.

### Western Blot Analysis of the Total and Immunoprecipitated Proteins of MDCK Cells

Samples containing 20  $\mu$ L of the MDCK cell extract mixed with 20  $\mu$ L of SDS–PAGE sample buffer or 10–30  $\mu$ L of proteins eluted from the protein A- or G-conjugated agarose beads were loaded onto 4 to 12% gradient SDS–PAGE gels (Invitrogen). Proteins were separated by SDS–PAGE using MES/SDS running buffer [0.05 M MES, 0.05 M Tris base, 0.1% SDS, and 1 mM EDTA (pH 7.3)], transferred onto a nitrocellulose membrane (Bio-Rad), and detected by Western blot analysis using the appropriate primary antibody and the anti-mouse or anti-rabbit IgG conjugated to alkaline phosphatase (Promega) as a secondary antibody. Alkaline phosphatase was detected using nitro blue tetrazolium and 5-bromo-4-chloro-3-indolyl phosphate in alkaline phosphatase buffer [150 mM NaCl and 1 mM MgCl<sub>2</sub> in 10 mM Tris-HCl (pH 9.0)]. Immunoblots were quantified by densitometry using Zeiss LSM 510, version 3.2.

### Trypsin Digestion

The susceptibility of the mutated and wild-type Na,K-ATPase  $\beta$  subunits to the limited tryptic digest was used to assess the effect of mutations on folding of the subunit. Wild-type YFP- $\beta_1$ , wild-type YFP- $\beta_2$ , and the unglycosylated mutant of YFP- $\beta_1$  are predominantly located on the plasma membrane of MDCK cells and, hence, contain complex-type or hybrid-type N-glycans. However, the glycosylation-deficient mutant of YFP- $\beta_2$ , D12458, is largely retained in the ER and, therefore, contains only high-mannose N-glycans. To prevent heterogeneity in N-glycan sizes, cells were treated with 100  $\mu$ g/mL deoxymannojirimycin, an  $\alpha$ -mannosidase 1 inhibitor, for 48 h prior to the trypsin digest experiment. Deoxymannojirimycin prevents processing of ER high-mannose chains to complex- and hybrid-type chains in the Golgi; as a result, all newly synthesized N-glycans become high-mannose-type glycans. Incubation with the inhibitor for 48 h was found to be sufficient to replace the vast majority of the existing YFP-linked  $\beta$  subunits with the newly synthesized high-mannose-type glycosylated forms of the subunits.

The monolayers of deoxymannojirimycin-treated cells were rinsed twice with ice-cold PBS and lysed via incubation with 200  $\mu$ L of 150 mM NaCl in 50 mM Tris (pH 7.5) containing 1% Nonidet P40 and 0.5% sodium deoxycholate. The protein concentration in cell lysates was determined using the BCA assay kit (Pierce) and adjusted to 3 mg/mL. Cell lysates were incubated with trypsin, which was added in the concentration range of 0–3  $\mu$ g/mL as indicated at 37 °C for 30 min. The reaction was stopped by the addition of 20  $\mu$ g/mL trypsin inhibitor (Sigma-Aldrich) and incubation of samples on ice for 10 min. Then, samples

containing 20  $\mu$ L of the reaction mixture combined with 20  $\mu$ L of SDS-PAGE sample buffer were incubated at 80 °C for 5 min, subjected to 4–12% SDS-PAGE, and analyzed by Western blotting by using a monoclonal anti-YFP antibody.

### Homology Modeling of the Na,K-ATPase $\beta_2$ Subunit

Model building was performed with Insight II and Discover software from Accelrys Inc. (San Diego, CA), utilizing the consistent valence force field. A homology model for the human Na,K-ATPase  $\beta_2$  subunit structure was generated by a combination of side chain replacement and loop rebuilding starting with the dogfish Na,K-ATPase  $\beta_1$  subunit structure file contained within Protein Data Bank (PDB) entry 2zxe (34). Side chain replacement for nonconserved residues was guided by a ClustalW multiple-sequence alignment matching the target human Na,K-ATPase  $\beta_2$  subunit to dogfish and pig Na,K-ATPase  $\beta_1$  subunits, the human Na,K-ATPase  $\beta_3$  subunit, and pig and rabbit H,K-ATPase  $\beta$  subunits. Initial side chain dihedral angles before energy minimization were assigned to nonconserved residues on the basis of the allowed ranges found in high-resolution structures such that no van der Waals overlap was given with neighboring conserved side chains in either the  $\alpha$  or  $\beta$  subunits. Nonconserved loop replacements were made by searching a database of loop structures contained in the Searchloop module of the software for loops with the desired number of amino acids that also matched the secondary structure in the conserved regions before and after the loop. After nonconserved loop and side chain replacement, the model was energy minimized with conserved side chains and internal secondary structures, including disulfide bonds, held fixed. Energy minimization was conducted to an average absolute derivative of less than 0.01 kcal mol<sup>-1</sup> Å<sup>-1</sup> with a fixed dielectric constant of 15, and a 15 Å nonbonded cutoff to generate the final model in the figure.

### Statistical Analysis

This was performed using a Student's *t* test (GraphPad Prism 4 and Microsoft Excel). Statistical significance is specified in the figure legends.

## RESULTS

### Expressed $\beta_1$ and $\beta_2$ Subunits Colocalize with the Endogenous $\alpha_1$ Subunit in the Plasma Membrane

In nontransfected MDCK cells, the major endogenous Na,K-ATPase subunit isoforms are  $\alpha_1$  and  $\beta_1$ , and these are predominantly located on the lateral membrane (35). Exogenously expressed YFP-linked  $\beta_1$  and  $\beta_2$  subunits are also largely colocalized with the endogenous  $\alpha_1$  subunit in the lateral membranes of confluent monolayers of MDCK cells (Figure 1). Intracellular retention of YFP- $\beta_1$  is negligible, while a minor fraction of YFP- $\beta_2$  is seen inside the cells (Figure 1).

### N-Glycosylation Is Essential for Maturation of the $\beta_2$ but Not the $\beta_1$ Subunit

It has been shown previously that removal of N-glycosylation sites from the Na,K-ATPase  $\beta_1$  subunit only slightly affects its delivery to the plasma membrane (16). Thus, mutagenic removal of one or two of the three N-glycosylation sites has almost no effect on the plasma membrane location of the subunit, while mutation of all three sites in YFP- $\beta_1$  results in minor intracellular accumulation in MDCK cells (16).

However, the unglycosylated mutant of YFP- $\beta_2$  is found largely inside the cells (Figure 2A, left) colocalized with the fluorescent marker of the ER (Figure 2B), indicating that the mutant is unable to traffic to the Golgi. YFP- $\beta_2$  is also retained in the ER in cells incubated in the presence of the N-glycosylation inhibitor, tunicamycin (Figure 2A, right), confirming

that it is the lack of N-glycans, not just the multiple amino acid substitutions in the unglycosylated mutant, that results in ER retention of YFP- $\beta_2$ .

To determine whether maturation of the  $\beta_1$  and  $\beta_2$  subunits depends on interaction of its N-glycans with the ER lectins, we incubated cells expressing YFP- $\beta_1$  or YFP- $\beta_2$  with the glucosidase inhibitor, castanospermine. Since calnexin binds to nascent glycoproteins only after progressive removal of two glucose residues from N-glycans by ER glucosidases I and II, castanospermine prevents interaction of N-glycans with calnexin (Figure 3A). Incubation of cells with castanospermine results in minor ER retention of YFP- $\beta_1$  but almost complete ER retention of YFP- $\beta_2$  (Figure 3B), showing that N-glycans contribute to folding and maturation of the subunits via interaction with calnexin.

### **Calnexin Interacts More Efficiently with the $\beta_2$ Subunit Than with the $\beta_1$ Subunit**

Expression of either YFP- $\beta_1$  or YFP- $\beta_2$  in MDCK cells does not change the amount of calnexin in total cell lysates (Figure 4A, bottom panel, lanes 4–6). Consistently, the amount of calnexin precipitated by a polyclonal antibody against calnexin is similar in nontransfected MDCK cells and cells expressing either YFP- $\beta_1$  or YFP- $\beta_2$  (Figure 4A, bottom panel, lanes 1–3). Also, the cellular content of the non-lectin chaperone, BiP, does not change (not shown), indicating that expression of YFP- $\beta_1$  or YFP- $\beta_2$  does not generate ER stress.

In total cell lysates, both YFP- $\beta_1$  and YFP- $\beta_2$  are detected as two bands. The higher band represents the mature complex-type glycosylated fraction of each subunit (Figure 4A, top panel, lanes 5 and 6, C), and the lower band represents the high-mannose-type glycosylated fraction (Figure 4A, top panel, lanes 5 and 6, H) (22). The high-mannose-type glycosylated subunits are immature forms resident in the ER, while the complex-type glycosylated subunits that can be formed only in the Golgi are mature forms that are mostly resident in the plasma membrane (22).

The complex-type forms of both YFP- $\beta_1$  and YFP- $\beta_2$  run more slowly than their corresponding high-mannose forms in SDS-PAGE, reflecting the increase in N-glycan size due to elongation and branching by the Golgi-resident glycosidases. If this increase in size were the same for the N-glycans of the two subunits, the difference in the gel mobility of the complex-type and high-mannose forms of YFP- $\beta_2$  (eight N-glycans) would be greater than that of YFP- $\beta_1$  (three N-glycans). However, this difference is even smaller in YFP- $\beta_2$  than in YFP- $\beta_1$  (Figure 4A, C), indicating that, on average, N-glycans of the  $\beta_2$  subunit undergo less elongation and branching in the Golgi than the N-glycans of the  $\beta_1$  subunit.

Immunoprecipitation using a polyclonal calnexin antibody results in coprecipitation of both YFP- $\beta_1$  and YFP- $\beta_2$  (Figure 4A, top panel, lanes 2 and 3). Both YFP- $\beta_1$  and YFP- $\beta_2$  assemble with the endogenous  $\alpha_1$  subunit in the ER in MDCK cells (22). However, the  $\alpha_1$  subunit does not coprecipitate with calnexin (Figure 4A, middle panel), indicating that calnexin binds to unassembled  $\beta$  subunits but not to the assembled  $\alpha$ - $\beta$  oligomers. Therefore, in contrast to several other oligomeric glycoproteins whose oligomerization is controlled by calnexin (36, 37), calnexin is involved in folding and quality control of only unassembled Na,K-ATPase  $\beta$  subunits, but not of the  $\alpha$ - $\beta$  complex.

Only the ER-resident high-mannose forms of both YFP- $\beta_1$  and YFP- $\beta_2$  coprecipitated with calnexin, consistent with the known ER location of calnexin. The amount of coprecipitated YFP- $\beta_2$  normalized to the amount of total high-mannose YFP- $\beta_2$  in a cell lysate is ~7-fold greater than the normalized amount of coprecipitated YFP- $\beta_1$  (Figure 4B).

A more efficient binding of calnexin to the  $\beta_2$  subunit than to the  $\beta_1$  subunit is confirmed in co-immunoprecipitation experiments performed in a converse manner. A polyclonal anti-YFP antibody coprecipitates calnexin with both YFP- $\beta_1$  and YFP- $\beta_2$  (Figure 4C, lanes 1 and 2). No coprecipitation of calnexin is detected with unglycosylated mutants of YFP- $\beta_1$  and YFP- $\beta_2$  (Figure 4C, lanes 3 and 4), indicating that calnexin binds to the N-glycans attached to YFP- $\beta_1$  and YFP- $\beta_2$ . The amount of calnexin that coprecipitates with YFP- $\beta_2$  is 6.3-fold greater than the amount of YFP- $\beta_1$ -bound calnexin shown by normalization of the density of the calnexin bands to the density of the high-mannose YFP- $\beta$  bands (Figure 4D).

YFP- $\beta_1$ -bound calnexin is detected before but not after incubation of the cell with cycloheximide for 1 h (Figure 4E, left panels). In contrast, association of YFP- $\beta_2$  with calnexin is retained even after incubation of the cell with cycloheximide 5 h (Figure 4E, right panels).

### Roles of Individual N-Glycans in Folding, Assembly with the $\alpha$ Subunit, and ER Export of the $\beta_2$ Subunit

To determine which of the eight N-glycans are important for  $\beta_2$  subunit maturation, N-glycosylation sites were mutated either individually or together with other(s) in various combinations. The location and numbering of N-glycosylation sites in the human  $\beta_2$  subunit aligned with the rat  $\beta_1$  subunit are schematically shown in Figure 5A. N-Glycosylation site mutants are named with a “D” followed by the number of the N-glycosylation sites removed by mutations (D1, D2, D12458, etc.). Western blot analysis of total lysates of the cells expressing YFP- $\beta_2$  with individual or multiple mutations of N-glycosylation sites shows the expected stepwise decrease in the relative molecular weight of the mutants that correlates with the number of sites removed (Figure 1 of the Supporting Information), showing that all eight putative N-glycosylation sites of the human  $\beta_2$  subunit are occupied by N-glycans.

There is a differential response resulting from N-glycan site deletions. The majority of single N-glycosylation site mutations, D1, D3–D6, and D8, have no effect on the plasma membrane localization of the  $\beta_2$  subunit (Figure 5B). However, the absence of the N-glycan at position 7 results in partial retention of the subunit in the ER. Removal of N-glycosylation site 7 in combination with site 2 results in full intracellular retention of the  $\beta_2$  subunit (Figure 5B, D7 and D27). As expected, multiple mutations of sites 1, 2, 3, 6, and 7 also result in complete intracellular retention of the subunit (Figure 5B, D12367).

The removal of only site 2 results in minor intracellular retention of the  $\beta_2$  subunit (Figure 5B, D2), and double mutations of site 2 together with site 1 or site 3 result in full intracellular retention of the subunit (Figure 5B, D12 and D23). However, the mutant lacking sites 1 and 3 is mostly in the plasma membrane (Figure 5B, D13). Removal of sites 4, 5, and 8 largely preserves plasma membrane localization of YFP- $\beta_2$  and only slightly increases the level of intracellular accumulation (Figure 5B, D458). The mutants with four sites deleted (sites 3, 4, 5, and 8) and even with five sites deleted (sites 3, 4, 5, 6, and 8) also preserve partial plasma membrane location (Figure 5B, D3458 and D34568). However, additional removal of site 7 or simultaneous mutation of sites 1, 2, 4, 5, and 8 results in full intracellular retention of the  $\beta_2$  subunit (Figure 5B, D345678, and Figure 6C). All the mutants that are retained inside the cells have an ER location. As an example, Figure 6A shows colocalization of the D12 mutant with the ER marker.

Assembly with the  $\alpha_1$  subunit is required for exit of the  $\beta_2$  subunit from the ER (22). To determine whether the ER retention of N-glycosylation-deficient mutants is due to their impaired ability to assemble with the  $\alpha_1$  subunit, we evaluated interaction of the mutants with the  $\alpha_1$  subunit by precipitating YFP-linked mutants using an anti-YFP antibody. Immunoprecipitation of wild-type YFP- $\beta_2$  results in coprecipitation of the  $\alpha_1$  subunit (Figure

6B, left lane). However, no coprecipitation of the  $\alpha_1$  subunit is detected with the mutants retained in the ER, such as the D27 mutant shown as an example (Figure 6B, right lane). In addition, all the ER-retained mutants, such as D12458, are not colocalized with the  $\alpha_1$  subunit as detected by immunostaining of the  $\alpha_1$  subunit (Figure 6C). To determine whether these mutants lose the ability to assemble with the  $\alpha_1$  subunit due to misfolding, limited tryptic digestion of selected mutants was performed in comparison with that of the wild type. The D12458 mutant is more susceptible to trypsin digestion (Figure 6D,E), suggesting that its proper conformation is not achieved after these mutations.

### Roles of Individual N-Glycans of the $\beta_2$ Subunit in Interaction of the Subunit with the ER Chaperones

To determine the roles of individual N-glycans in folding and quality control of the  $\beta_2$  subunit in the ER, we tested selected N-glycosylation site mutants for interaction with BiP and calnexin. Stronger binding of the mutants to a non-lectin ER chaperone, BiP, that is known to interact with terminally misfolded glycoproteins should indicate the impairment of folding by mutations, while mutation-induced changes in calnexin binding should reflect the contribution of individual N-glycans to calnexin-assisted folding.

The binding of BiP to the  $\beta_2$  subunit is strengthened because of mutations D12, D27, D458, D4568, and D12458 (Figure 7) but is not affected by single mutations of site 2 or site 7 (Figure 8A). Calnexin binding is dramatically weakened due to the D27 mutation (Figures 7 and 8A). However, the amount of subunit-bound calnexin is only slightly decreased by individual removal of site 7 and is not affected by removal of site 2 (Figure 8A). On the other hand, the level of co-immunoprecipitated calnexin is increased due to D12, D458, D4568, and D12458 mutations (Figure 7).

The presence of hydrophobic amino acid clusters in the vicinity of N-glycosylation sites is known to affect post-translational calnexin binding (7,8,38,39). Hydropathy analysis (40) of the  $\beta_2$  subunit amino acid sequence shows the presence of a conserved relatively hydrophobic stretch of amino acids, <sup>243</sup>LVAVKFL, following site 7 (Figure 2 of the Supporting Information). In contrast, the regions following the other N-glycosylation sites in the  $\beta_2$  subunit and three sites in the  $\beta_1$  subunit are more hydrophilic (Figure 2 of the Supporting Information). Hydrophilic substitution of one hydrophobic residue in the region C-terminal to N-glycosylation site 7 in combination with mutation of N-glycosylation site 2, D2-L249T, slightly decreases the hydrophobicity of the region but does not affect the plasma membrane location of the subunit or calnexin binding (not shown). However, mutation of two or three hydrophobic residues in this region to hydrophilic residues in combination with mutation of N-glycosylation site 2, D2-V244/Q-L249T (D2-VL/QT) and D2-L243Q-V244Q-L249T (D2-LVL/QQT), results in a progressive decrease in the hydrophobicity of the region (Figure 8B), full ER retention of the  $\beta_2$  subunit (Figure 8C), a significant increase in the level of BiP binding, and a large decrease in the level of calnexin binding (Figure 8A). Hydrophilic substitutions for two hydrophobic residues even in the wild-type subunit, V244Q-L249T (VL/QT), result in a significant decrease in the level of calnexin binding, an increase in the level of BiP binding, and full ER retention of the  $\beta_2$  subunit (Figure 8). In contrast, hydrophobic substitution for the lysine residue, K247L, in the same region does not change calnexin or BiP binding and preserves the plasma membrane location of the  $\beta_2$  subunit (Figure 8), emphasizing the importance of the hydrophobic residues in this locus for normal subunit maturation.

## DISCUSSION

### Diverse Functions of N-Glycans Linked to the $\beta$ Subunits of the Na,K-ATPase and H,K-ATPase

N-Glycans as bulky hydrophilic structural elements of glycoproteins are important for stabilization of their proper tertiary structure. They also play diverse roles in protein maturation, trafficking, signaling, and cell adhesion, which often require the contribution of different lectins (5–9). Here we show that N-glycans are crucial for lectin-mediated folding and quality control of the  $\beta_2$  subunit but not of the  $\beta_1$  subunit of the Na,K-ATPase.

Previous studies have shown that N-glycans of the  $\beta$  subunits of the Na,K-ATPase and the homologous gastric H,K-ATPase responsible for the secretion of acid by the parietal cell of the stomach are also important for the post-ER trafficking of these enzymes, as well as for intercellular adhesion and cell migration. Five of the eight N-glycans of the Na,K-ATPase  $\beta_2$  subunit that are unique to this subunit appear to be important for apical sorting of the subunit in gastric HGT-1 cells (33). Similarly, all seven N-glycans of the H,K-ATPase  $\beta$  subunit are important for apical sorting of this subunit in LLC-PK1 cells (32). In contrast, the three N-glycans of the Na,K-ATPase  $\beta_1$  subunit, while not required for plasma membrane delivery, are important for the lateral membrane retention of the pump due to glycan-mediated interaction between  $\beta_1$  subunits of neighboring cells in cell monolayers and cytosolic linkage of the  $\alpha$  subunit to the cytoskeleton (16). In addition, its N-glycans contribute to the formation of cell–cell contacts between surface-attached dispersed MDCK cells by mediating lamellipodia formation and stabilizing the newly formed adherens junctions (16). Also, the structure of the N-glycans of this subunit is important for intercellular adhesion and cell migration. Further, epithelial cells can regulate the tightness of cell junctions and cell motility via glycosyltransferase remodeling of N-glycans, including those linked to the Na,K-ATPase  $\beta_1$  subunit (17). The roles of interactions of the  $\beta$  subunit N-glycans with lectins in apical sorting, plasma membrane retention, intercellular adhesion, and cell migration remain to be elucidated.

### The $\beta_2$ Subunit, but Not the $\beta_1$ Subunit, Undergoes Post-Translational Calnexin-Assisted Folding

Prevention of N-glycosylation of the Na,K-ATPase  $\beta_2$  subunit by tunicamycin or by mutation of eight N-glycosylation sites results in full retention of the subunit in the ER (Figure 2). The ER retention of the N-glycosylation-deficient  $\beta_2$  subunit is also associated with an increased sensitivity of the subunit to limited tryptic digestion (Figure 6D,E) and loss of  $\alpha$ – $\beta$  assembly (Figure 6B,C), suggesting that the lack of N-glycans impairs correct subunit folding. Consistently, the ER retention of N-glycosylation-deficient mutants correlates with enhanced binding to BiP (Figure 7) that is known to interact with misfolded glycoproteins. Therefore, N-glycans are essential for normal folding and maturation of this subunit isoform.

Incubation of cells with castanospermine that prevents calnexin binding to N-glycans (41) results in almost complete retention of the  $\beta_2$  subunit in the ER (Figure 3B, right panel), indicating that interactions of N-glycans with calnexin are important for normal trafficking of the  $\beta_2$  subunit. Indeed, the wild-type  $\beta_2$  subunit, but not its unglycosylated mutant, binds to calnexin (Figure 4C, lanes 2 and 4).

Similar to the  $\beta_2$  subunit, the homologous  $\beta_1$  subunit of the Na,K-ATPase binds calnexin in an N-glycan-dependent manner (Figure 4C, lanes 1 and 3). When all three N-glycans are present, but their interaction with calnexin is prevented by castanospermine, the  $\beta_1$  subunit is partially retained in the ER (Figure 3B, left panel), showing that calnexin–glycan interactions also contribute to the normal maturation of this subunit. In contrast to the  $\beta_2$

subunit whose interaction with calnexin persists for at least 5 h after translation has stopped, the interaction of the  $\beta_1$  subunit with calnexin disappears after incubation of the cells with cycloheximide for only 1 h (Figure 4E). These data indicate that the  $\beta_2$  subunit continues to bind to calnexin after the completion of translation, while the  $\beta_1$  subunit presumably binds calnexin mostly cotranslationally. Accordingly, at steady state, the amount of  $\beta_2$ -bound calnexin is 6–7-fold greater than the amount of  $\beta_1$ -bound calnexin (Figure 4A–D). Also, the ER residence time is much greater for the  $\beta_2$  subunit than for the  $\beta_1$  subunit as seen from the different rates of decrease in the amount of the high-mannose forms of the two subunits in the absence of protein synthesis (Figure 4E).

In addition to lectin chaperones, the  $\beta_1$  subunit presumably employs non-lectin ER chaperones for its folding. Indeed, the  $\beta_1$  subunit has been found to interact with BiP (26) and wolframin (42). These non-lectin chaperones presumably assist in the maturation of the nonglycosylated  $\beta_1$  subunit to allow its exit from the ER and trafficking to the plasma membrane (16).

ER lectin chaperones are known to slow protein folding, thus improving folding efficiency and fidelity (5,6). In contrast to the ubiquitously expressed Na,K-ATPase  $\beta_1$  subunit, the  $\beta_2$  subunit is expressed in only a few tissues and is most abundant in brain and muscle. In addition to its role as a subunit of the ion pumping enzyme, the  $\beta_2$  subunit plays an important role in adhesion and migration of glial cells (14). The level of expression of the  $\beta_2$  subunit has been found to be decreased in various types of gliomas (43,44). It is likely that the Na,K-ATPase  $\beta_2$  subunit needs to achieve a particular conformation to perform its specific functions and hence has to undergo stricter quality control in the ER.

### N-Glycans 7 and 2 and the Hydrophobic Amino Acid Cluster in the Proximity of These N-Glycans Are Essential for Calnexin-Mediated Folding of the $\beta_2$ Subunit

A comparison of the results of individual and multiple mutations of N-glycosylation sites shows that there appears to be a hierarchical importance of the N-glycans for the exit of the  $\beta_2$  subunit from the ER. N-Glycan 7 appears to be the most critical for trafficking to the plasma membrane, because its removal alone results in significant retention of the subunit in the ER, while individual mutations of other sites result in minor retention or no retention (Figure 5B). N-Glycan 2 appears to be less significant than N-glycan 7, since individual removal of site 2 results only in less intracellular retention of the  $\beta_2$  subunit. Double mutations of site 2 together with site 1 or 3 result in full ER retention of the subunit, but the mutant lacking sites 1 and 3 is still mostly in the plasma membrane (Figure 5B). Therefore, the N-glycan at position 2 is more relevant to normal maturation of the  $\beta_2$  subunit as compared to N-glycan 1 or 3. Also, N-glycans 4, 5, 6, and 8 are likely less important than N-glycans 7 and 2, since partial plasma membrane localization of the subunit is preserved in the D34568 mutant (Figure 5B).

Normal trafficking of the  $\beta_2$  subunit is impaired by cell incubation with castanospermine (Figure 3), indicating that interactions of N-glycans with the ER lectins contribute to correct folding of the  $\beta_2$  subunit. On the other hand, a minor fraction of the  $\beta_2$  subunit reaches the plasma membrane in castanospermine-treated cells (Figure 3B, right panel), in contrast to full ER retention of the unglycosylated subunit (Figure 2) and particular N-glycosylation site-deficient mutants (Figure 5B). Therefore, N-glycans are important for maturation of the  $\beta_2$  subunit not only because of their interaction with the ER folding-promoting lectins but also because of their direct contribution to the correct conformation. The presence of bulky polar carbohydrate chains can modify the properties of the polypeptide, thus affecting its secondary or tertiary structure and stability of folding intermediates (45–47).

Mutations of N-glycosylation site 7 alone result in a moderate decrease in the level of calnexin binding, while simultaneous removal of sites 7 and 2 results in a large decrease in the level of calnexin binding. In contrast, all other individual or multiple N-glycosylation site mutations that preserve site 7 and/or site 2 do not change or even increase the amount of subunit-bound calnexin (Figure 7). These results indicate that N-glycans 7 and 2 are the preferred sites for calnexin binding to the  $\beta_2$  subunit.

The basis for preferential employment of selected N-glycans by the ER lectin chaperone system is poorly understood. Two factors appear to be important, the relative position of the N-glycans in the protein and the amino acid sequence of the regions flanking an N-glycosylation site.

The presence of N-glycans within ~50 N-terminal luminal amino acid residues has been shown to be critical for cotranslational binding of calnexin to a number of glycoproteins (5,48). The N-terminal location of N-glycan 2 (Figure 5A) might suggest the involvement of this glycan in cotranslational calnexin-assisted folding of the  $\beta_2$  subunit. However, N-glycan 1 that is located even closer to the N-terminus than N-glycan 2 appears to be less important than N-glycan 2 for the ER exit of the subunit as is seen from the full ER retention of D23 but with the major plasma membrane location of D13 (Figure 5B).

It is not clear whether specific amino acid motifs are important for cotranslational calnexin binding. However, post-translational calnexin binding seems to depend on the protein sequence in the vicinity of a specific N-glycan. The ER-resident enzyme UGGT1 acts as a sensor of the conformation of deglycosylated glycoproteins released from calnexin (7,8). UGGT1 binds to hydrophobic amino acid patches exposed on the surface of incompletely folded glycoproteins and adds back a glucose residue to the proximal N-glycan(s), allowing another cycle of calnexin binding and, hence, continued calnexin-mediated refolding (38,39) (Figure 3A).

The  $\beta_2$  subunit contains a conserved relatively hydrophobic region of amino acids downstream from N-glycan 7 (Figure 2 of the Supporting Information). Mutations of two or three hydrophobic residues in this region to hydrophilic residues in combination with mutation of N-glycosylation site 2 result in full ER retention of the  $\beta_2$  subunit, a large decrease in the level of calnexin binding, and a significant increase in the level of BiP binding (Figure 8) similar to that seen in the D27 mutant. Therefore, hydrophilic mutations after N-glycosylation site 7 in the D2 mutant mimic the absence of N-glycan 7. These results suggest that the  $\beta_2$  subunit encounters prolonged calnexin binding through N-glycan 7, possibly due to reglycosylation of this N-glycan by UGGT1, allowing repeated calnexin cycling.

In support of this hypothesis, D12, D458, D4568, and D12458 mutants bind more calnexin than the wild-type subunit does (Figure 7). The increased extent of co-immunoprecipitation of calnexin in spite of the fewer N-glycans in these mutants as compared to the wild-type subunit must be due to an increased duration of subunit–calnexin interaction. Presumably, the lack of N-glycans in these mutants impairs correct folding of the subunit, which results in additional calnexin-mediated folding attempts. The presence of N-glycan 7 in all these mutants is consistent with the contribution of N-glycan 7 to UGGT1-induced post-translational calnexin binding.

Homology modeling of the three-dimensional structure of the  $\beta_2$  subunit based on a high-resolution structure of the Na,K-ATPase consisting of  $\alpha_1$  and  $\beta_1$  subunits shows that N-glycan 2 is adjacent to N-glycan 7 and to the hydrophobic residues C-terminal to N-glycan 7 in the folded subunit (Figure 9). Hydrophilic substitutions for two hydrophobic residues downstream from N-glycan 7 in the wild-type  $\beta_2$  subunit with all N-glycosylation sites

intact result in a significant decrease in the level of calnexin binding, an increase in the level of BiP binding, and full ER retention of the subunit, similar to that found in the D27 mutant. Hence, this mutation of hydrophobic residues resembles the absence of both N-glycans 7 and 2, but not the absence of just N-glycan 7 (Figures 5B and 8).

The results suggest that surface exposure of these hydrophobic residues in an incompletely folded wild-type subunit results in UGGT1-catalyzed reglucosylation of both N-glycans 7 and 2. As a result, either N-glycan 2 or N-glycan 7 can bind calnexin for post-translational refolding of the subunit. In the absence of one of these two N-glycans, calnexin still can bind to the other, allowing post-translational folding of the  $\beta_2$  subunit and export from the ER. This interpretation explains why individual removal of either N-glycosylation site 7 or N-glycosylation site 2 does not prevent calnexin binding or export of the subunit from the ER (Figures 5B and 8A).

However, when both N-glycans 2 and 7 are absent, reglucosylation does not happen and the  $\beta_2$  subunit does not bind calnexin post-translationally and, hence, cannot acquire native conformation, which results in the ER retention of the subunit (Figures 5B and 7). Similarly, reglucosylation, post-translational calnexin-mediated folding, and export of the subunit from the ER are impaired due to mutation of the hydrophobic residues near N-glycan 7 that are presumably required for UGGT1 binding (Figure 8).

However, a possibility that the hydrophobic residues next to site 7 are important for calnexin–subunit binding per se cannot be excluded. Also, full ER retention of the V244Q-L249T (VL/QT) mutant versus only partial ER retention of the  $\beta_2$  subunit in castanospermine-treated cells indicates that this mutation also has a direct effect on folding in addition to disruption of glycan–calnexin interaction.

Correct folding of the  $\beta_2$  subunit is required for its assembly with the  $\alpha_1$  subunit, which, in turn, is necessary for exit of both subunits from the ER (22). Of the eight N-glycans of the  $\beta_2$  subunit, N-glycans 2 and 7 are the closest to the 7–8 extracellular loop of the  $\alpha_1$  subunit that is the main site of the association with the  $\beta_2$  subunit (34,49) (Figure 9A), perhaps accounting for the critical role of these glycans in maturation of the subunit and its export from the ER.

In conclusion, N-glycans are crucial for maturation of the Na,K-ATPase  $\beta_2$  subunit, but not of the  $\beta_1$  subunit. Two N-glycans, 7 and 2, present in the  $\beta_2$  subunit, but not in the  $\beta_1$  subunit, are essential for calnexin-mediated folding and quality control of the former subunit. The hydrophobic residues in the proximity of these N-glycans are required for the post-translational calnexin-assisted maturation of the  $\beta_2$  subunit.

## Supplementary Material

Refer to Web version on PubMed Central for supplementary material.

## Acknowledgments

We are thankful to Mark Doolittle and Osnat Ben-Zeev for advice and critical comments.

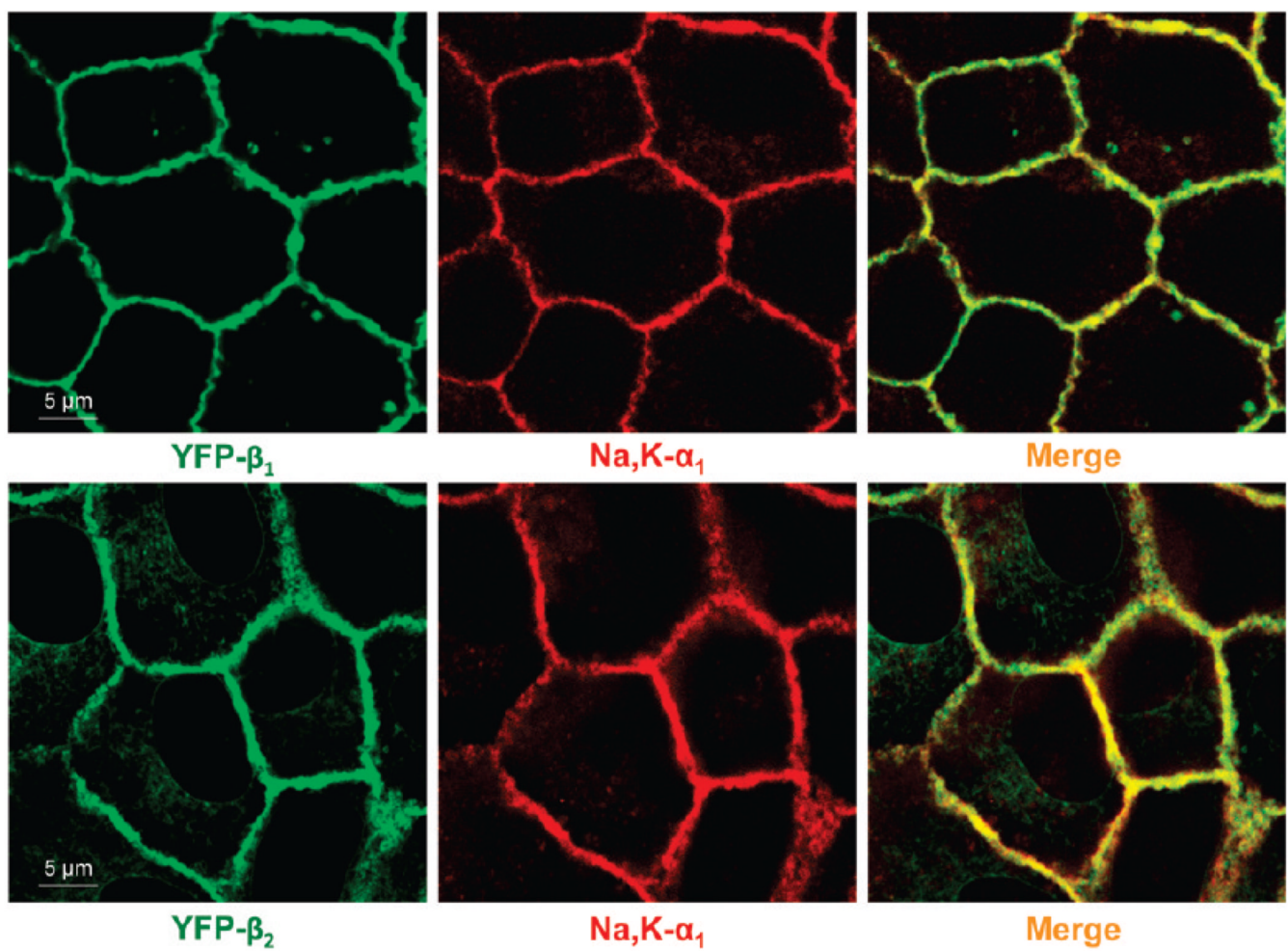
## REFERENCES

1. Meusser B, Hirsch C, Jarosch E, Sommer T. ERAD: The long road to destruction. *Nat. Cell Biol.* 2005; 7:766–772. [PubMed: 16056268]
2. Romisch K. Endoplasmic reticulum-associated degradation. *Annu. Rev. Cell Dev. Biol.* 2005; 21:435–456. [PubMed: 16212502]

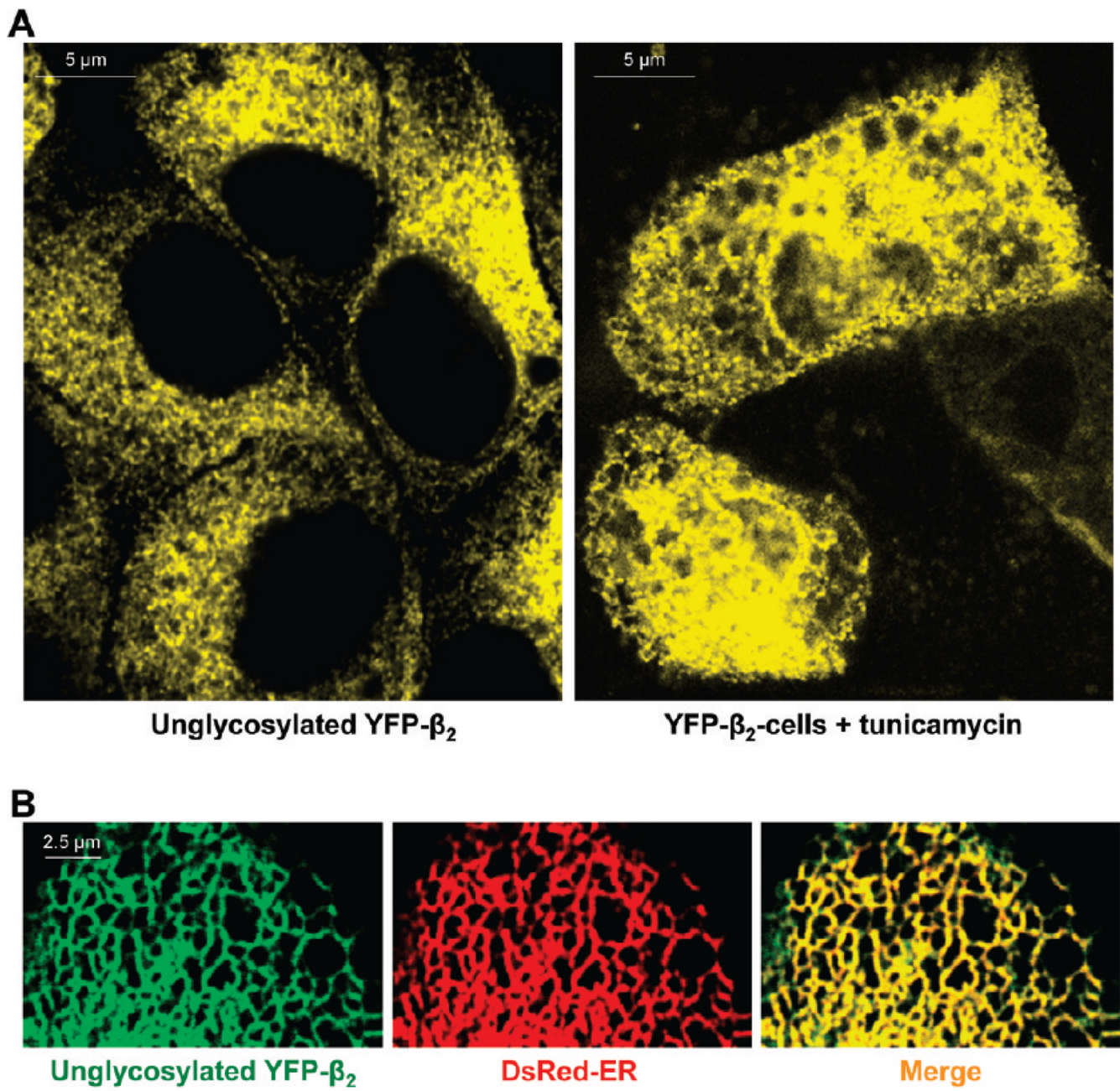
3. McCracken AA, Brodsky JL. Evolving questions and paradigm shifts in endoplasmic-reticulum-associated degradation (ERAD). *BioEssays*. 2003; 25:868–877. [PubMed: 12938176]
4. Kreplak L, Aebi U. From the polymorphism of amyloid fibrils to their assembly mechanism and cytotoxicity. *Adv. Protein Chem.* 2006; 73:217–233. [PubMed: 17190615]
5. Hebert DN, Molinari M. In and out of the ER: Protein folding, quality control, degradation, and related human diseases. *Physiol. Rev.* 2007; 87:1377–1408. [PubMed: 17928587]
6. Ruddock LW, Molinari M. N-Glycan processing in ER quality control. *J. Cell Sci.* 2006; 119:4373–4380. [PubMed: 17074831]
7. Caramelo JJ, Parodi AJ. How sugars convey information on protein conformation in the endoplasmic reticulum. *Semin. Cell Dev. Biol.* 2007; 18:732–742. [PubMed: 17997334]
8. Caramelo JJ, Parodi AJ. Getting in and out from calnexin/calreticulin cycles. *J. Biol. Chem.* 2008; 283:10221–10225. [PubMed: 18303019]
9. Helenius A, Aebi M. Roles of N-linked glycans in the endoplasmic reticulum. *Annu. Rev. Biochem.* 2004; 73:1019–1049. [PubMed: 15189166]
10. Solda T, Galli C, Kaufman RJ, Molinari M. Substrate-specific requirements for UGT1-dependent release from calnexin. *Mol. Cell.* 2007; 27:238–249. [PubMed: 17643373]
11. Molinari M, Galli C, Vanoni O, Arnold SM, Kaufman RJ. Persistent glycoprotein misfolding activates the glucosidase II/UGT1-driven calnexin cycle to delay aggregation and loss of folding competence. *Mol. Cell.* 2005; 20:503–512. [PubMed: 16307915]
12. Xie Z. Molecular mechanisms of Na/K-ATPase-mediated signal transduction. *Ann. N.Y. Acad. Sci.* 2003; 986:497–503. [PubMed: 12763870]
13. Tian J, Xie ZJ. The Na-K-ATPase and calcium-signaling microdomains. *Physiology*. 2008; 23:205–211. [PubMed: 18697994]
14. Gloor S, Antonicek H, Sweadner KJ, Pagliusi S, Frank R, Moos M, Schachner M. The adhesion molecule on glia (AMOG) is a homologue of the  $\beta$  subunit of the Na,K-ATPase. *J. Cell Biol.* 1990; 110:165–174. [PubMed: 1688561]
15. Rajasekaran SA, Barwe SP, Gopal J, Ryazantsev S, Schneeberger EE, Rajasekaran AK. Na-K-ATPase regulates tight junction permeability through occludin phosphorylation in pancreatic epithelial cells. *Am. J. Physiol.* 2007; 292:G124–G133.
16. Vagin O, Tokhtaeva E, Sachs G. The role of the  $\beta_1$  subunit of the Na,K-ATPase and its glycosylation in cell-cell adhesion. *J. Biol. Chem.* 2006; 281:39573–39587. [PubMed: 17052981]
17. Vagin O, Tokhtaeva E, Yakubov I, Shevchenko E, Sachs G. Inverse correlation between the extent of N-glycan branching and intercellular adhesion in epithelia. Contribution of the Na,K-ATPase  $\beta_1$  subunit. *J. Biol. Chem.* 2008; 283:2192–2202. [PubMed: 18025087]
18. Geering K. Functional roles of Na,K-ATPase subunits. *Curr. Opin. Nephrol. Hypertens.* 2008; 17:526–532. [PubMed: 18695395]
19. Blanco G, Mercer RW. Isozymes of the Na-K-ATPase: Heterogeneity in structure, diversity in function. *Am. J. Physiol.* 1998; 275:F633–F650. [PubMed: 9815123]
20. Crambert G, Hasler U, Beggah AT, Yu C, Modyanov NN, Horisberger JD, Lelievre L, Geering K. Transport and pharmacological properties of nine different human Na, K-ATPase isozymes. *J. Biol. Chem.* 2000; 275:1976–1986. [PubMed: 10636900]
21. Noguchi S, Mishina M, Kawamura M, Numa S. Expression of functional ( $\text{Na}^+ + \text{K}^+$ )-ATPase from cloned cDNAs. *FEBS Lett.* 1987; 225:27–32. [PubMed: 2826244]
22. Tokhtaeva E, Sachs G, Vagin O. Assembly with the Na,K-ATPase  $\alpha_1$  subunit is required for export of  $\beta_1$  and  $\beta_2$  subunits from the endoplasmic reticulum. *Biochemistry*. 2009; 48:11421–11431. [PubMed: 19764716]
23. Geering K. The functional role of  $\beta$  subunits in oligomeric P-type ATPases. *J. Bioenerg. Biomembr.* 2001; 33:425–438. [PubMed: 11762918]
24. Noguchi S, Higashi K, Kawamura M. A possible role of the  $\beta$ -subunit of (Na,K)-ATPase in facilitating correct assembly of the  $\alpha$ -subunit into the membrane. *J. Biol. Chem.* 1990; 265:15991–15995. [PubMed: 2168428]

25. Noguchi S, Higashi K, Kawamura M. Assembly of the  $\alpha$ -subunit of *Torpedo californica*  $\text{Na}^+/\text{K}^+$ -ATPase with its pre-existing  $\beta$ -subunit in *Xenopus* oocytes. *Biochim. Biophys. Acta.* 1990; 1023:247–253. [PubMed: 2158350]
26. Beggah AT, Jaunin P, Geering K. Role of glycosylation and disulfide bond formation in the  $\beta$  subunit in the folding and functional expression of  $\text{Na},\text{K}$ -ATPase. *J. Biol. Chem.* 1997; 272:10318–10326. [PubMed: 9092584]
27. Zamofing D, Rossier BC, Geering K. Inhibition of N-glycosylation affects transepithelial  $\text{Na}^+$  but not  $\text{Na}^+/\text{K}^+$ -ATPase transport. *Am. J. Physiol.* 1989; 256:C958–C966. [PubMed: 2541620]
28. Laughery MD, Todd ML, Kaplan JH. Mutational analysis of  $\alpha$ - $\beta$  subunit interactions in the delivery of  $\text{Na},\text{K}$ -ATPase heterodimers to the plasma membrane. *J. Biol. Chem.* 2003; 278:34794–34803. [PubMed: 12826673]
29. Tamkun MM, Fambrough DM. The ( $\text{Na}^+ + \text{K}^+$ )-ATPase of chick sensory neurons. Studies on biosynthesis and intracellular transport. *J. Biol. Chem.* 1986; 261:1009–1019. [PubMed: 3003048]
30. Takeda K, Noguchi S, Sugino A, Kawamura M. Functional activity of oligosaccharide-deficient ( $\text{Na},\text{K}$ )ATPase expressed in *Xenopus* oocytes. *FEBS Lett.* 1988; 238:201–204. [PubMed: 2844594]
31. Lian WN, Wu TW, Dao RL, Chen YJ, Lin CH. Deglycosylation of  $\text{Na}^+/\text{K}^+$ -ATPase causes the basolateral protein to undergo apical targeting in polarized hepatic cells. *J. Cell Sci.* 2006; 119:11–22. [PubMed: 16339171]
32. Vagin O, Turdikulova S, Sachs G. The  $\text{H},\text{K}$ -ATPase  $\beta$  subunit as a model to study the role of N-glycosylation in membrane trafficking and apical sorting. *J. Biol. Chem.* 2004; 279:39026–39034. [PubMed: 15247221]
33. Vagin O, Turdikulova S, Sachs G. Recombinant addition of N-glycosylation sites to the basolateral  $\text{Na},\text{K}$ -ATPase  $\beta 1$  subunit results in its clustering in caveolae and apical sorting in HGT-1 cells. *J. Biol. Chem.* 2005; 280:43159–43167. [PubMed: 16230337]
34. Shinoda T, Ogawa H, Cornelius F, Toyoshima C. Crystal structure of the sodium-potassium pump at 2.4 Å resolution. *Nature.* 2009; 459:446–450. [PubMed: 19458722]
35. Dunbar LA, Courtois-Coutry N, Roush DL, Muth TR, Gottardi CJ, Rajendran V, Geibel J, Kashgarian M, Caplan MJ. Sorting of P-type ATPases in polarized epithelial cells. *Acta Physiol. Scand., Suppl.* 1998; 643:289–295. [PubMed: 9789572]
36. Tomita Y, Yamashita T, Sato H, Taira H. Kinetics of interactions of sendai virus envelope glycoproteins, F and HN, with endoplasmic reticulum-resident molecular chaperones, BiP, calnexin, and calreticulin. *J. Biochem.* 1999; 126:1090–1100. [PubMed: 10578061]
37. Keith N, Parodi AJ, Caramelo JJ. Glycoprotein tertiary and quaternary structures are monitored by the same quality control mechanism. *J. Biol. Chem.* 2005; 280:18138–18141. [PubMed: 15746090]
38. Ritter C, Quirin K, Kowarik M, Helenius A. Minor folding defects trigger local modification of glycoproteins by the ER folding sensor GT. *EMBO J.* 2005; 24:1730–1738. [PubMed: 15861139]
39. Taylor SC, Thibault P, Tessier DC, Bergeron JJ, Thomas DY. Glycopeptide specificity of the secretory protein folding sensor UDP-glucose glycoprotein:glucosyltransferase. *EMBO Rep.* 2003; 4:405–411. [PubMed: 12671684]
40. Kyte J, Doolittle RF. A simple method for displaying the hydropathic character of a protein. *J. Mol. Biol.* 1982; 157:105–132. [PubMed: 7108955]
41. Hammond C, Braakman I, Helenius A. Role of N-linked oligosaccharide recognition, glucose trimming, and calnexin in glycoprotein folding and quality control. *Proc. Natl. Acad. Sci. U.S.A.* 1994; 91:913–917. [PubMed: 8302866]
42. Zatyka M, Ricketts C, da Silva Xavier G, Minton J, Fenton S, Hofmann-Thiel S, Rutter GA, Barrett TG. Sodium-potassium ATPase 1 subunit is a molecular partner of Wolframin, an endoplasmic reticulum protein involved in ER stress. *Hum. Mol. Genet.* 2008; 17:190–200. [PubMed: 17947299]
43. van den Boom J, Wolter M, Blaschke B, Knobbe CB, Reifenberger G. Identification of novel genes associated with astrocytoma progression using suppression subtractive hybridization and real-time reverse transcription-polymerase chain reaction. *Int. J. Cancer.* 2006; 119:2330–2338. [PubMed: 16865689]

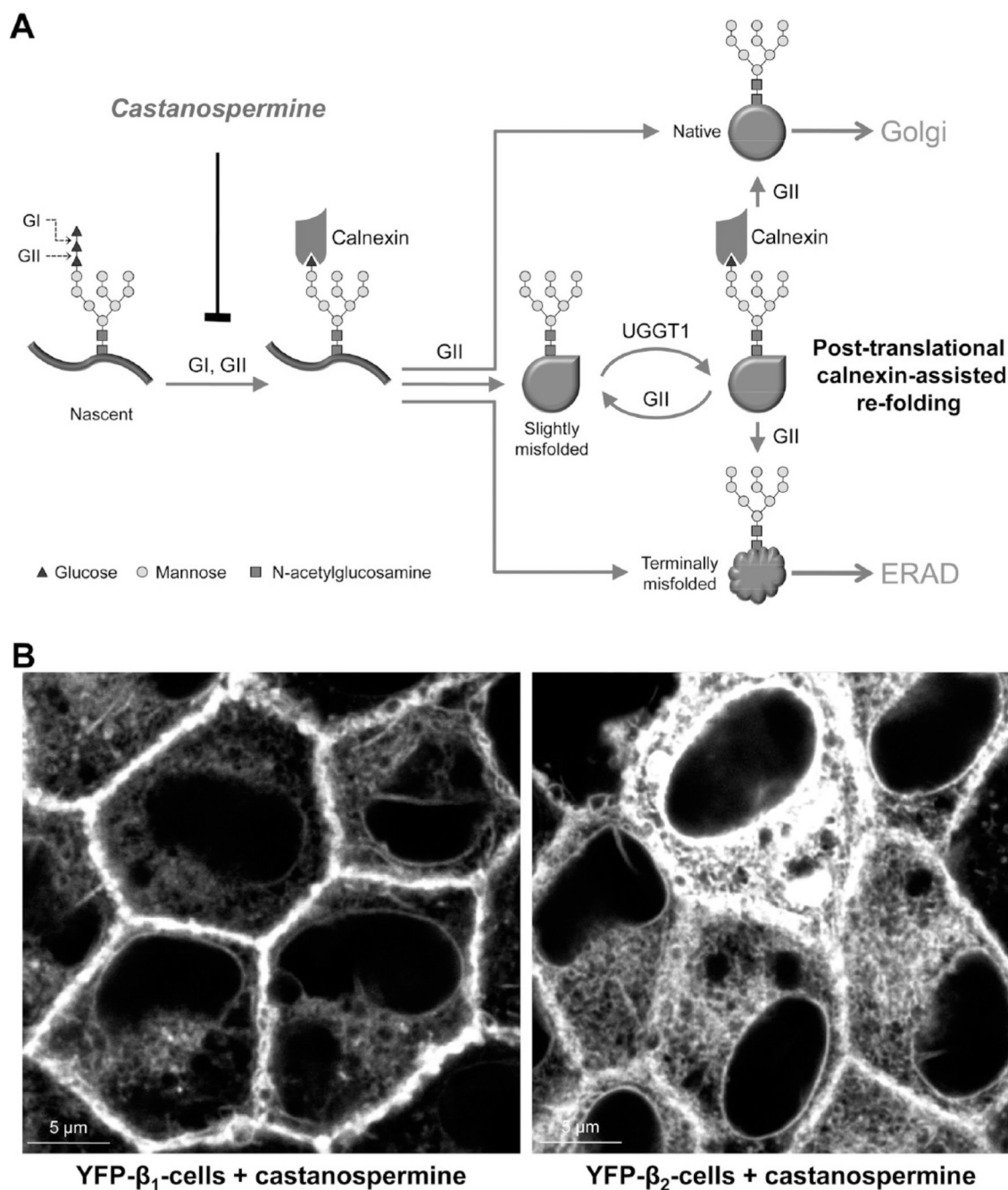
44. Senner V, Schmidtpeter S, Braune S, Puttmann S, Thanos S, Bartsch U, Schachner M, Paulus W. AMOG/ $\beta$ 2 and glioma invasion: Does loss of AMOG make tumour cells run amok? *Neuropathol. Appl. Neurobiol.* 2003; 29:370–377. [PubMed: 12887597]
45. Bosques CJ, Tschampel SM, Woods RJ, Imperiali B. Effects of glycosylation on peptide conformation: A synergistic experimental and computational study. *J. Am. Chem. Soc.* 2004; 126:8421–8425. [PubMed: 15237998]
46. Petrescu AJ, Milac AL, Petrescu SM, Dwek RA, Wormald MR. Statistical analysis of the protein environment of N-glycosylation sites: Implications for occupancy, structure, and folding. *Glycobiology.* 2004; 14:103–114. [PubMed: 14514716]
47. Imperiali B, O'Connor SE. Effect of N-linked glycosylation on glycopeptide and glycoprotein structure. *Curr. Opin. Chem. Biol.* 1999; 3:643–649. [PubMed: 10600722]
48. Molinari M, Helenius A. Chaperone selection during glycoprotein translocation into the endoplasmic reticulum. *Science.* 2000; 288:331–333. [PubMed: 10764645]
49. Colonna TE, Huynh L, Fambrough DM. Subunit interactions in the Na,K-ATPase explored with the yeast two-hybrid system. *J. Biol. Chem.* 1997; 272:12366–12372. [PubMed: 9139681]

**FIGURE 1.**

YFP-linked Na,K-ATPase  $\beta_1$  and  $\beta_2$  subunits of the Na,K-ATPase colocalize with the endogenous Na,K-ATPase  $\alpha_1$  subunit. Confocal microscopy images showing that YFP- $\beta_1$  and YFP- $\beta_2$  (green) colocalize with the endogenous Na,K-ATPase  $\alpha_1$  subunit (red) in the lateral membranes of MDCK cells as detected by immunostaining of cells expressing YFP- $\beta_1$  or YFP- $\beta_2$  using monoclonal antibody against the Na,K-ATPase  $\alpha_1$  subunit.

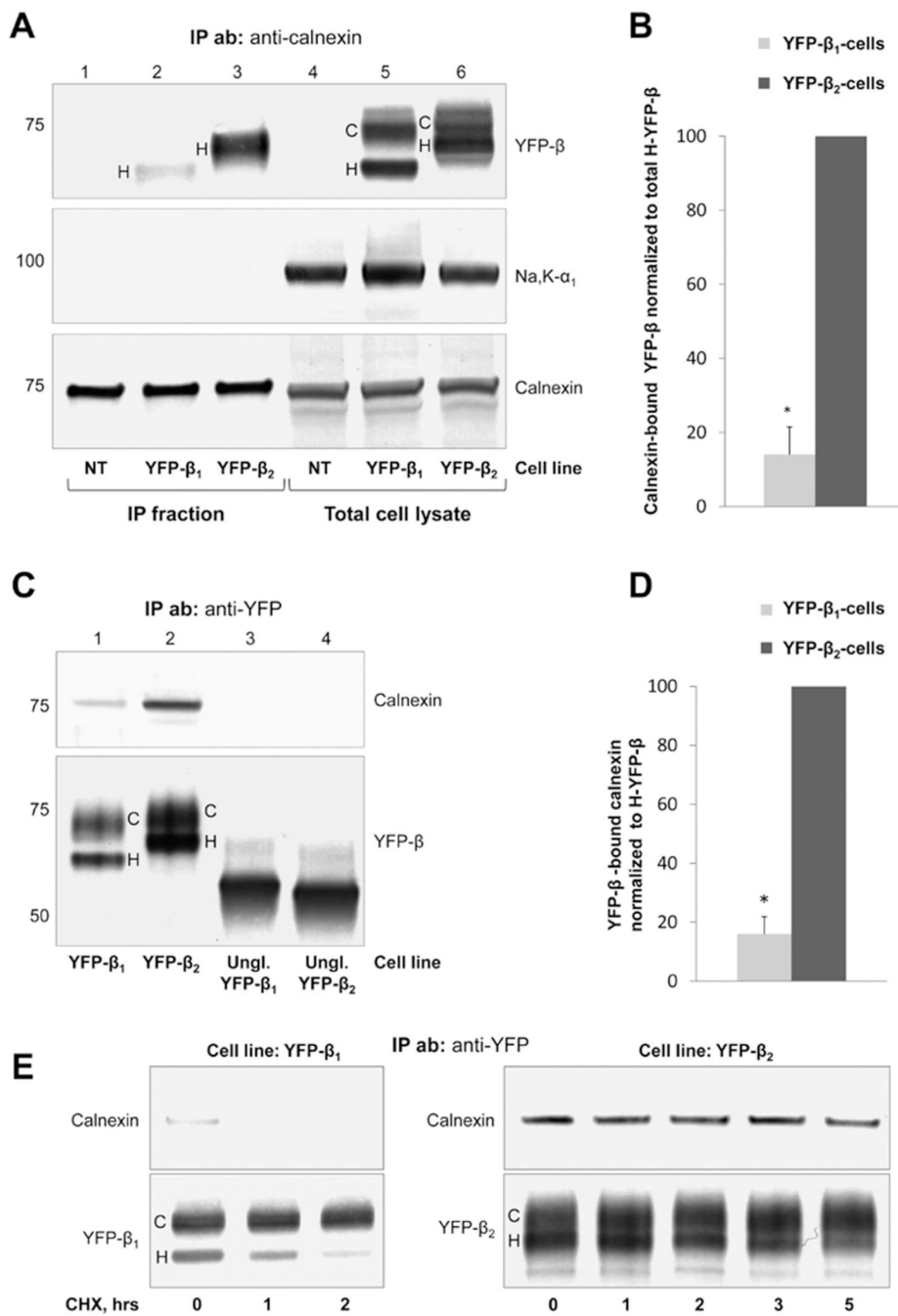
**FIGURE 2.**

Unglycosylated Na,K-ATPase  $\beta_2$  subunit retained in the ER. (A) Confocal microscopy images of MDCK cells show intracellular retention of YFP- $\beta_2$  due to prevention of N-glycosylation either by mutagenesis of all eight N-glycosylation sites (left) or by incubation of cells expressing wild-type YFP- $\beta_2$  with 1  $\mu$ g/mL tunicamycin for 48 h (right). (B) The unglycosylated mutant of YFP- $\beta_2$  (green) is colocalized with the ER (red) as detected by transient expression of the fluorescent ER marker, DsRed2-ER, in the mutant-expressing cells.

**FIGURE 3.**

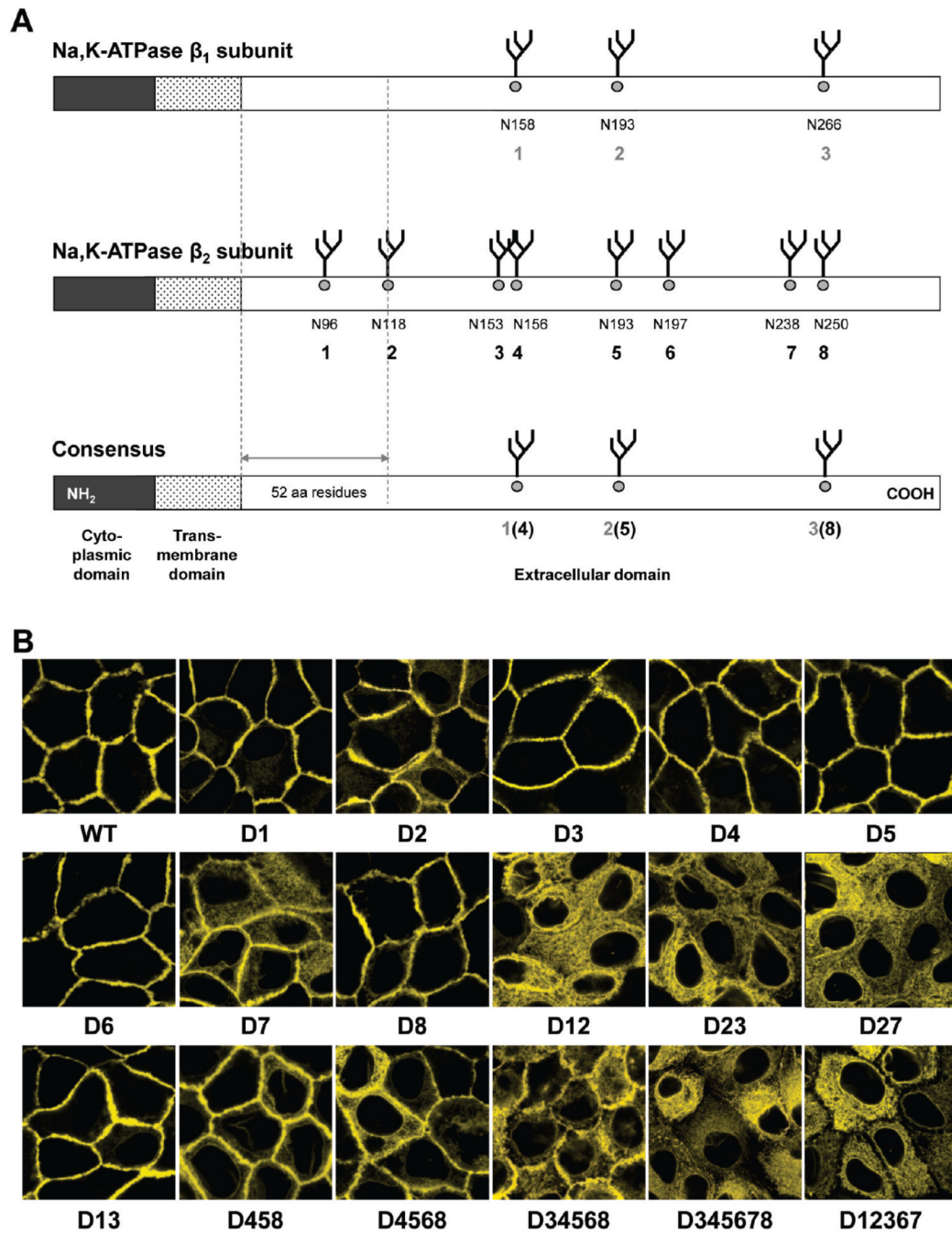
Maturation of both  $\beta_1$  and  $\beta_2$  subunits of the Na,K-ATPase depends on interaction of their N-glycans with calnexin. (A) Schematic presentation of cotranslational and post-translational calnexin binding to glycoproteins. N-Glycans are added cotranslationally to the asparagine residue within the N-glycosylation site of a nascent protein. Removal of two of the three glucose residues by glucosidases I and II (GI and GII, respectively) enables cotranslational binding of N-glycan to calnexin. Removal of the last glucose by GII releases glycoprotein from calnexin. If glycoprotein is folded correctly, it is exported to Golgi. If the protein is terminally misfolded, it is translocated to the cytoplasm for the ER-associated degradation (ERAD). If the protein is slightly misfolded, it is reglucosylated by UDP-

glucose glycoprotein glucosyltransferase 1 (UGGT1) and binds again to calnexin for refolding. Removal of glucose residues and, hence, calnexin binding can be blocked by castanospermine. (B) Incubation of MDCK cells expressing either YFP- $\beta_1$  or YFP- $\beta_2$  with 1 mM castanospermine for 48 h results in minor ER retention of YFP- $\beta_1$  (left) and almost full ER retention of YFP- $\beta_2$  (right).

**FIGURE 4.**

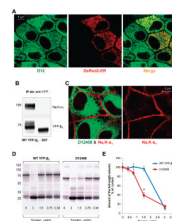
Calnexin interacts more efficiently with the unassembled β<sub>2</sub> subunit than with the unassembled β<sub>1</sub> subunit of the Na,K-ATPase. (A) The polyclonal antibody against calnexin precipitates calnexin (bottom panels) and coprecipitates YFP-β<sub>1</sub> and YFP-β<sub>2</sub> (top panels) but does not coprecipitate the Na,K-ATPase α<sub>1</sub> subunit (middle panels) from the total lysates of YFP-β<sub>1</sub>- and YFP-β<sub>2</sub>-expressing cells. No co-immunoprecipitation is detected in nontransfected cells (NT). Monoclonal antibodies against calnexin, YFP, and the Na,K-ATPase α<sub>1</sub> subunit were used for Western blot analysis. (B) Densitometry quantification of the results shown in panel A indicates that the amount of coprecipitated YFP-β<sub>2</sub> normalized to the amount of total high-mannose YFP-β<sub>2</sub> in a cell lysate is 7-fold greater than the

normalized amount of calnexin-reacting YFP- $\beta_1$ . (C) A polyclonal antibody against YFP precipitates YFP- $\beta_1$ , YFP- $\beta_2$  and unglycosylated mutants of YFP- $\beta_1$  and YFP- $\beta_2$  (bottom panel) from respective total cell lysates. Calnexin is coprecipitated with YFP- $\beta_1$  and YFP- $\beta_2$ , but not with their unglycosylated mutants (top panel). Monoclonal antibodies against calnexin and YFP were used for Western blot analysis. (D) Densitometric quantification of the results shown in panel C indicates that the amount of co-immunoprecipitated calnexin normalized to the amount of immunoprecipitated high-mannose YFP- $\beta$  in the corresponding cell line is 6.3-fold higher in YFP- $\beta_2$ -expressing cells than in YFP- $\beta_1$ -expressing cells. (E) YFP- $\beta_1$  or YFP- $\beta_2$  was immunoprecipitated before or after incubation of YFP- $\beta_1$ - or YFP- $\beta_2$ -expressing cells with 20  $\mu$ g/mL cycloheximide for the indicated periods of time using a polyclonal antibody against YFP. Immunoprecipitated YFP- $\beta_1$  and YFP- $\beta_2$  and co-immunoprecipitated calnexin were analyzed by Western blot analysis using monoclonal antibodies against calnexin and YFP. YFP- $\beta_1$ -bound calnexin is detected before but not after incubation with cycloheximide for 2 h. Association of YFP- $\beta_2$  with calnexin is retained during the incubation of the cell with cycloheximide for 5 h. Error bars show the standard deviation ( $n = 3$ ). Asterisks denote a significant difference with “YFP- $\beta_2$  cells” ( $P < 0.01$ , Student’s  $t$  test). IP ab represents the antibody used for immunoprecipitation, IP fraction the immunoprecipitated fraction, Na,K- $\alpha_1$  the endogenous  $\alpha_1$  subunit of the Na,K-ATPase, C complex-type YFP- $\beta$ , and H high-mannose YFP- $\beta$ .

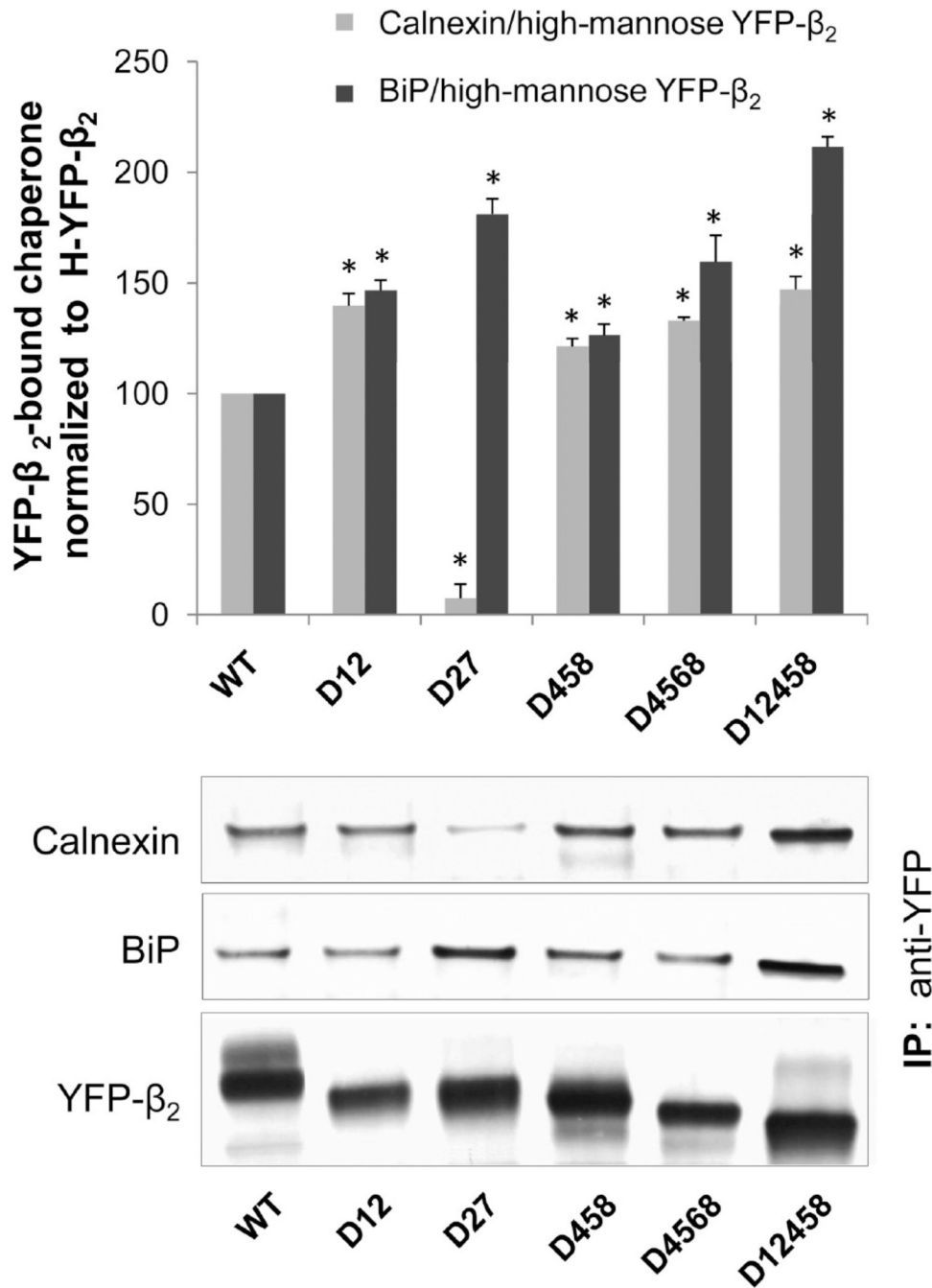
**FIGURE 5.**

Not all eight N-glycans are equally important for the export of the  $\beta_2$  subunit from the ER. (A) The primary structures of the Na,K-ATPase  $\beta_1$  and  $\beta_2$  subunits are drawn schematically and compared on the basis of the computational alignment (Vector NTI, version 8.0) of the rat  $\beta_1$  subunit (GenBank accession number NM\_013113) and the human  $\beta_2$  subunit (GenBank accession number NM\_001678). Numbers indicate asparagine residues of N-glycosylation sites (N158, N193, etc.) and the numbering of N-glycan positions used in the text (1–8). (B) Confocal microscopy images of MDCK cells expressing selected N-glycosylation-deficient mutants of YFP- $\beta_2$  show that the N-glycan at position 7 is the most

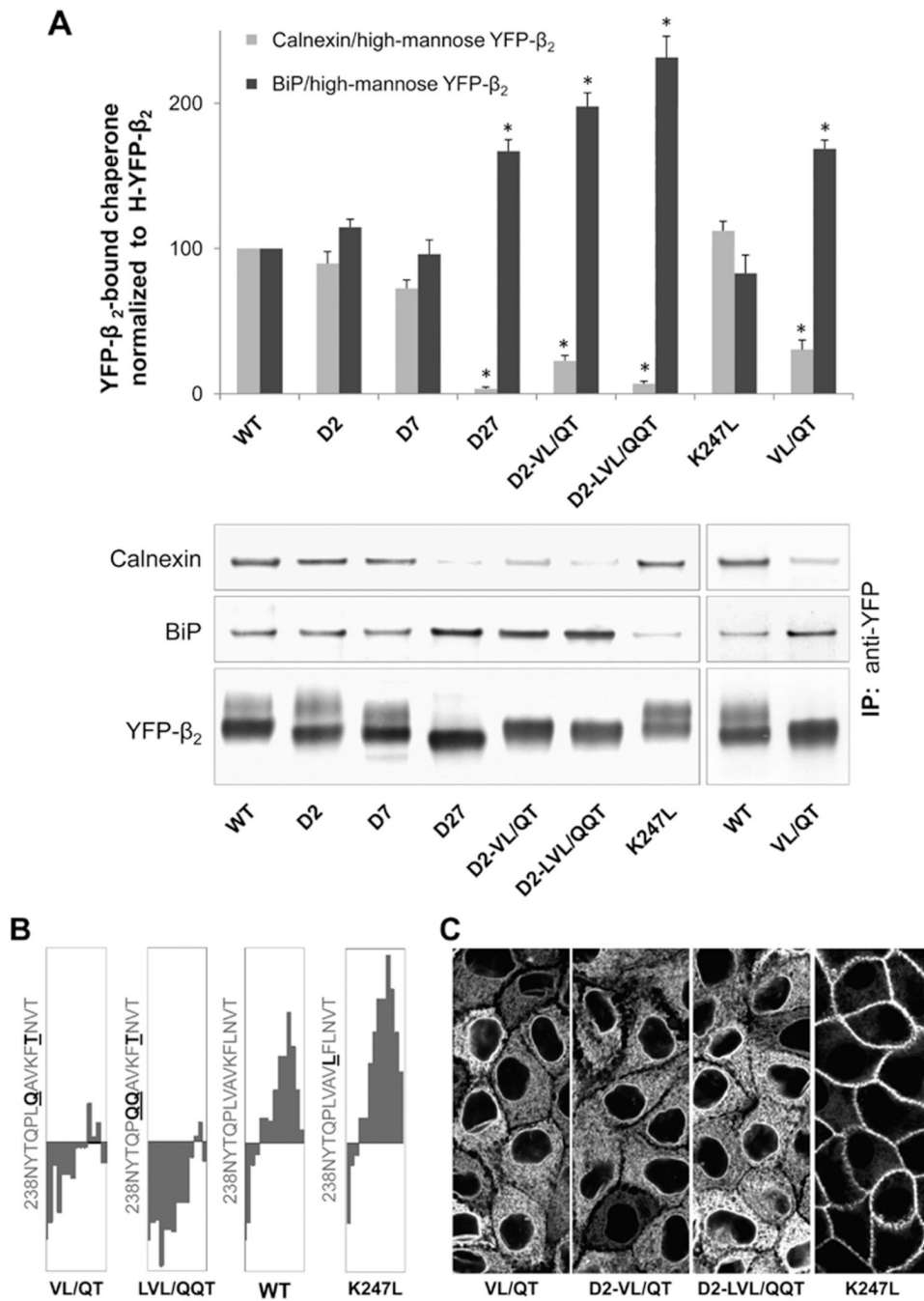
important for normal trafficking of the subunit to the plasma membrane, while the N-glycan at position 2 is less important than N-glycan 7, but more important than the other N-glycans.

**FIGURE 6.**

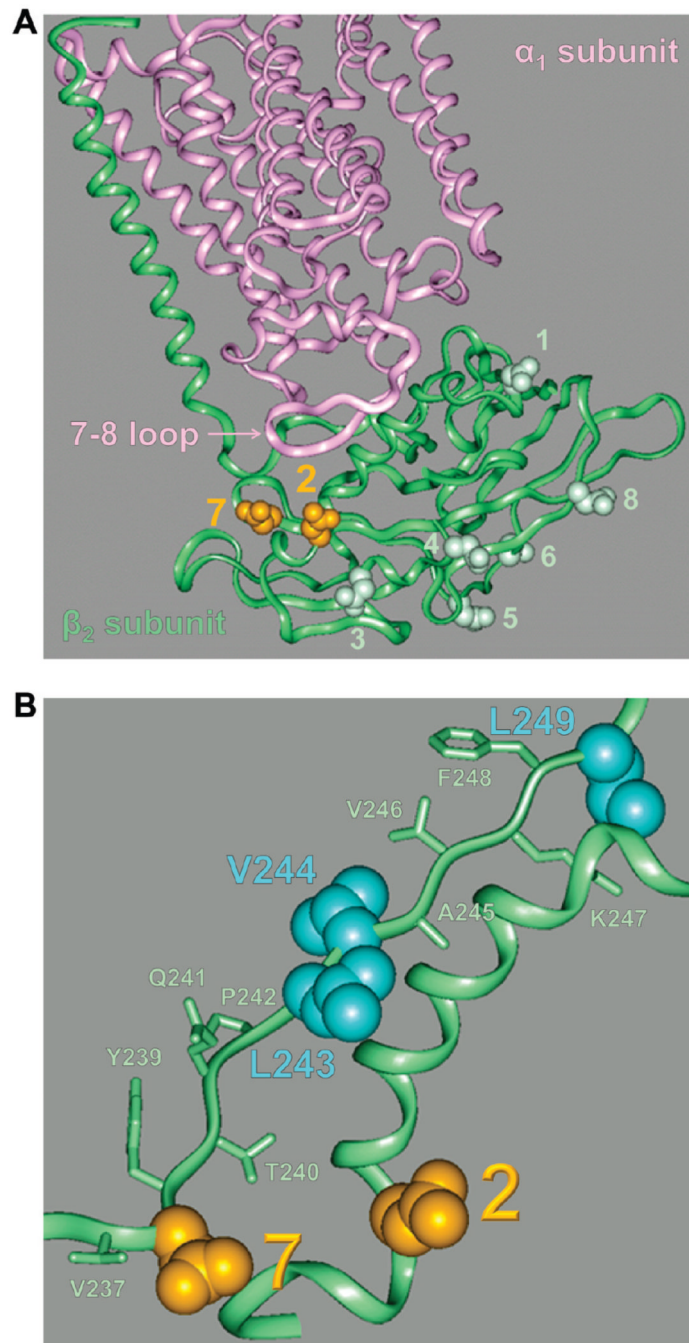
Mutation of particular N-glycosylation sites in the  $\beta_2$  subunit of the Na,K-ATPase impairs normal folding of the subunit and prevents its assembly with the  $\alpha_1$  subunit. (A) TheD12 mutant of YFP- $\beta_2$  (green) is colocalized with the ER(red) as detected by transient expression of the fluorescent ER marker, DsRed2-ER, in the mutant-expressing cells. (B) Wild-type YFP- $\beta_2$  and its D27 mutant were immunoprecipitated using a polyclonal antibody against YFP from the respective total cell lysates. Precipitated YFP-linked proteins (bottom) and the coprecipitated Na,K-ATPase  $\alpha_1$  subunit (top) were analyzed using monoclonal antibodies against YFP and the Na,K-ATPase  $\alpha_1$  subunit, respectively. The endogenous Na,K-ATPase  $\alpha_1$  subunit is coprecipitated with wild-type YFP- $\beta_2$ , but not with its D27 mutant. (C) The YFP-linked mutant of the  $\beta_2$  subunit, D12458, shows no colocalization with the  $\alpha_1$  subunit as detected by immunostaining of the mutant-expressing cells using the monoclonal antibody against the Na,K-ATPase  $\alpha_1$  subunit. (D) Confluent monolayers of the cells expressing either wild-type YFP- $\beta_2$  or its D12458 mutant were incubated in the presence of 100  $\mu$ g/mL deoxymannojirimycin, the inhibitor of N-glycan processing, for 48 h to prevent heterogeneity of N-glycans. After cell lysis, the whole cell lysates (3 mg/mL) were incubated without or with trypsin at the indicated concentration for 30 min. The products of tryptic digestion were analyzed by immunoblotting using the antibody against YFP. (E) Densitometric quantification of the full-length subunit band at various trypsin concentrations in three parallel experiments shown in panel D indicates that D12458 is more susceptible to digestion by trypsin than the wild-type subunit.

**FIGURE 7.**

Effect of glycosylation site mutations on binding of the Na,K-ATPase  $\beta_2$  subunit to calnexin and BiP. A monoclonal antibody against YFP precipitates wild-type YFP- $\beta_2$  (WT) and its glycosylation-deficient mutants (bottom) and co-immunoprecipitates calnexin and BiP from respective total cell lysates (top and middle). Polyclonal antibodies against YFP, calnexin, and BiP were used for Western blot analysis. Densitometry quantification of the results was performed via normalization of the density of the calnexin or BiP band to the density of the high-mannose YFP- $\beta_2$  band. Error bars show the standard deviation ( $n = 3$ ). Asterisks denote a significant difference with "WT" ( $P < 0.01$ , Student's  $t$  test).

**FIGURE 8.**

Effect of mutations in an amino acid region next to site 7 on binding of the β<sub>2</sub> subunit to calnexin and BiP, and on the ER to Golgi export. (A) Immunoprecipitation and Western blot analysis of wild-type YFP-β<sub>2</sub> (WT) and its mutants followed by densitometry quantification of the results were performed as described in the legend of Figure 7. (B) Fifteen-amino acid regions downstream of N-glycosylation site 7 (N238) of the hydropathy plots of the wild-type β<sub>2</sub> subunit and its mutants with a window size of 9 (40). (C) Confocal microscopy images of the mutant-expressing MDCK cells show full ER retention of the mutants with hydrophilic substitutions of hydrophobic residues and a plasma membrane location of the mutant with hydrophobic substitution of a hydrophilic residue.

**FIGURE 9.**

N-Glycan 2 is proximal to N-glycan 7 in the folded Na,K-ATPase  $\beta_2$  subunit. (A) A homology model of a three-dimensional structure of the Na,K-ATPase  $\beta_2$  subunit (green) associated with the  $\alpha_1$  subunit (pink) based on the high-resolution  $\alpha_1-\beta_1$  Na,K-ATPase structure (PDB entry 2zxe) shows asparagine residues of eight N-glycosylation sites of the  $\beta_2$  subunit in a space-filling view and the rest of the protein in a ribbon view. Asparagine residues of N-glycosylation sites 2 and 7 (orange) are located on the same side of the extracellular domain of the  $\beta_2$  subunit. (B) Magnified image of the Na,K-ATPase  $\beta_2$  subunit homology model showing the proximal location of the V237-L249 amino acid region to

both N-glycosylation sites 2 and 7 (orange). Hydrophobic residues subjected to hydrophilic substitutions via mutation (Figure 8) are colored blue.